

**Expression of TRPC1 and TRPC4 in the basilar artery after experimental subarachnoid hemorrhage in rats**Xiaoou Sun<sup>1</sup>, Shaofeng Yang<sup>2</sup>, Yuan Shi<sup>1</sup>, Chengyuan Ji<sup>1</sup>, Linyuan Wu<sup>1</sup>, Zhong Wang<sup>1\*</sup><sup>1</sup>Department of Neurosurgery, the First Affiliated Hospital of Soochow University, Suzhou, Jiangsu Province, China<sup>2</sup>Department of Neurosurgery, Taizhou No.2 Hospital of Traditional Chinese Medicine, Suzhou, Jiangsu Province, ChinaEmail: [Dr.zhongwang@gmail.com](mailto:Dr.zhongwang@gmail.com)

(Xiaoou Sun and Shaofeng Yang contributed equally to this work)

**Abstract: Objective:** This study investigated the expression of TRPC1 and TRPC4 in the basilar artery in a rat subarachnoid hemorrhage (SAH) model, and clarified the potential role of TRPC1 and TRPC4 in cerebral vasospasm. **Methods:** Seventy-two rats were randomized into six groups: control, day 1, day 3, day 5, day 7, and day 14 groups. The day 1, day 3, day 5, day 7, and day 14 groups were the SAH groups. The animals in the SAH groups were injected with autologous blood into the cisterna magna once on day 0, and were sacrificed on days 1, 3, 5, 7, and 14, respectively. The cross-sectional area of the basilar artery was measured, and morphological changes were detected using light microscopy. Immunohistochemistry, PCR, and western blotting were used to assess the expression of TRPC1 and TRPC4. **Results:** The rat “double-hemorrhage” model of vasospasm was successfully induced. The cross-sectional area of the basilar artery was  $57,944 \pm 5,581 \mu\text{m}^2$  in the control group, and  $32,100 \pm 2,439 \mu\text{m}^2$ ,  $19,723 \pm 2,412 \mu\text{m}^2$ ,  $26,100 \pm 2,639 \mu\text{m}^2$ ,  $34,800 \pm 2,580 \mu\text{m}^2$ , and  $57,100 \pm 2,579 \mu\text{m}^2$  in the day 1, 3, 5, 7, and 14 groups, respectively. The basilar artery exhibited vasospasm after SAH, which became more severe on day 3, and was characterized by arterial narrowing, thickness of arterial wall, and degeneration of the endothelial and smooth muscle cells. In addition, elevated expression of TRPC1 and TRPC4 were detected after SAH, and peaked on day 3. **Conclusion:** The increased expression of TRPC1 and TRPC4 mirrors the development of cerebral vasospasm in a rat experimental model of SAH. These findings suggest that TRPC1 and TRPC4 may have a role in the pathogenesis of cerebral vasospasm after SAH.

[Xiaoou Sun, Shaofeng Yang, Yuan Shi, Chengyuan Ji, Linyuan Wu, Zhong Wang. **Expression of TRPC1 and TRPC4 in the basilar artery after experimental subarachnoid hemorrhage in rats.** *Life Sci J* 2013; 10(3): 2665-2674]. (ISSN: 1097-8135). <http://www.lifesciencesite.com>. 385

**Key words:** Subarachnoid hemorrhage, Cerebral vasospasm,  $\text{Ca}^{2+}$ , TRPC1, TRPC4

**Introduction**

The annual incidence of spontaneous subarachnoid hemorrhage (subarachnoid hemorrhage, SAH) is approximately 6-16/100 000, accounting for 6-8% of the total incidence of stroke (Dumont et al., 2003; Ali et al., 2010; Gregory et al., 2011). The major cause of spontaneous SAH is rupture of an intracranial aneurysm. The occurrence of cerebral vasospasm (CVS) after aneurysmal SAH is a common complication, which can result in death (Kassell et al., 1990; Yahia et al., 2010; Christos, 2010). Although much basic and clinical research studying the pathogenesis of CVS has been carried out, its underlying mechanisms remain unclear. It is likely that CVS after SAH involves multiple causing factors. One theory suggests that subarachnoid hemorrhage is accompanied by the influx of a large number of calcium ions ( $\text{Ca}^{2+}$ ) into vascular endothelial cells and smooth muscle cells, activating a series of biological pathways and causing smooth muscle contraction (Dorsch, 1994; Harders et al., 1996; Ville et al., 2012). In recent years, the molecular mechanisms and signal transduction pathways that could be modulated to prevent CVS are gradually being

identified and characterized (Dietrich, 2000; Shigeru, 2005; Ricardo et al., 2007; Xu et al., 2010). Transient receptor cation channels (TRPC) are transmembrane proteins that allow transport across the cell membrane when activated, including calcium cations (Yao and Garland, 2005; Salgado and Ordaz, 2008; Yoon and Daejin, 2007; Daniela and Baruch, 2010). The function of vascular smooth muscle is partially regulated by calcium concentrations, and a variety of mechanisms can activate  $\text{Ca}^{2+}$  influx and cause intracellular  $\text{Ca}^{2+}$  concentrations to rise.

The present study reveals that  $\text{Ca}^{2+}$  flow is regulated by members of the super-family of TRPCs (Alexander and Vladimir, 2006; Geoffrey and Stewart, 2007; Ambudkar et al., 2013). We use the injection of autologous blood into the cisterna magna to establish a model of SAH, and then assessed the expression of TRPC1 and TRPC4 in basal artery at various time points to study the correlation and relationship between TRPC1 and TRPC4 levels with CVS after SAH.

**Aim:**

This study investigated the expression of

TRPC1 and TRPC4 in the basilar artery in a rat subarachnoid hemorrhage (SAH) model, and clarified the potential role of TRPC1 and TRPC4 in cerebral vasospasm.

## Materials and Methods

### Animal Models

Adult healthy male Sprague-Dawley (SD) rats weighing ~300-350 g were obtained from Soochow University of Medicine Laboratory Animal Research Center (Sue SYXK 2002-2012, cleanliness level 2). Animals were kept in single cage with an ambient temperature of 18-22°C, with free access to standard laboratory chow and water, in a quiet, dark environment. They were then randomly divided into the control, SAH1d, SAH3d, SAH5d, SAH7d, and SAH14d groups, with 12 rats per group, and any unexpected deaths were recorded. Rats in each SAH group were sacrificed on days 1, 3, 5, 7, and 14, as indicated. The control group was treated in the same way as the SAH groups except that they were injected with saline rather than autologous blood. At sacrifice, six rats per group were perfused and tissues fixed for morphological and immunohistochemical studies and the remaining six were used for protein extraction for analysis by western blotting.

### Blood injection in rats

The method of using cisterna magna blood injection to establish an SAH model has been previously described (Park and Joseph, 2008).

### Surgical Procedure

Animals anesthetized with an intraperitoneal injection of 10% chloral hydrate (0.35 ml/100 g), are fixed to the operating table in prone position. Three hundred microliters non-heparinized arterial blood was extracted from the tail artery, and slowly injected (over 2 min) into the cisterna magna subarachnoid. The rat was then kept in the prone position to allow the injected blood to accumulate around the basilar artery. In the control group, an equal volume of saline was injected into the Cisterna magna.

### Perfusion fixation materials and specimen

Animals were anesthetized using intraperitoneal injection of 10% chloral hydrate. The pericardium was opened to expose the heart and aortic root. Blood vessels were perfused with 0.1 mol/L PBS (pH 7.4), and the heart was then fixed with 4% paraformaldehyde in PBS. Samples for pathological and immunohistochemical examination were fixed in 4% paraformaldehyde for 24 h, while samples for protein analysis were flash frozen in liquid nitrogen.

### Basal artery morphology test and the determination of arterial diameter size

The entire basilar artery segment in fixed tissue blocks was divided into upper, middle and lower parts by separating 3 mm below the top of the basilar artery, in the middle of the basilar artery, and 3 mm at the bottom end of the basilar artery. Each part was traversed into a 2 mm long artery, which was paraffin-embedded with the brain stem. To compare the diameter of the arteries, the diameter of the circumference (over an average of three sections) was measured, and the mathematical formula  $\text{Area} = p^2/4\pi$  (where p is the perimeter) was used to calculate the diameter of the circular area using ImageJ (version 1.32) software.

### The phosphorylation of TRPC1 and TRPC4 in the basal artery wall, assessed by immunohistochemistry

Paraffin-embedded sections were dewaxed with xylene, and rinsed with distilled water. Antigen retrieval was then carried out in sodium citrate buffer pH 6.0. Slides were blocked using normal goat serum blocking solution, and then incubated with anti-TRPC1 (ab74819) or anti-TRPC4 antibody (ab63076) at a 1:100 dilution. Biotinylated goat anti-rabbit IgG was then added to each slide, followed by SABC and DAB reagents. The staining intensity was then assessed microscopically. Semi quantitative determination of the expression of TRPC1 and TRPC4 was then carried out, where 0 represents negative staining, and 1, 2, 3 and 4 represent the extent of positive staining, ranging from low, moderate, high, and very high. Fields were viewed at 400-x magnification.

### The mRNA expression of TRPC1 and TRPC4 in the basilar artery, assessed by RT-PCR

Real-time PCR was used to assess the expression of TRPC1 and 4 at an absorption of 497 nm, and an emission of 520 nm (Livak and Schmittgen, 2001; Liu and David, 2002). The following primers were used: Trpc1 (ID: 89821 NM\_053558.1 GI:25742644) rTrpc1F GCCAGCCCTTGAGAGAATAGAC and rTrpc1R TGTGTGAGCCACCACTTTGAG. Trpc4 (ID:84494) rTrpc4F ACCCCAGACATCACGCCTA and rTrpc4R TGGACCGTGAGTGCCTGAG; rat actin f(150) CCCATCTATGAGGGTTACGC and r(150) TTTAATGTCACGCACGATTTTC. RNA was extracted from fresh tissue samples using TRIzol reagent, following the manufacturer's instructions. qRT-PCR was then carried out on reaction mixes containing RT buffer, random primers, RT mix, and template cDNA. The cycles were as follows: 25°C for 10 min, 42°C degrees for 50 min, and 85°C for 5 min, followed by amplification with 35 cycles of 94°C for 4 min, 94°C for 20 sec, 60°C for 30 sec, and 72°C for 30 sec, before incubation at 72°C.

### Expression of TRCP1 and TRPC4 assessed by western blotting

Tissue extracts were homogenized in RIPA buffer, and quantified using Coomassie brilliant blue G250. Extracts were separated by SDS-PAGE and transferred to PVDF membranes. Membranes were then blocked, and incubated with primary antibodies, as indicated, washed, and incubated with secondary antibodies. After additional washes in TBST, bands were visualized using chemiluminescence.

### Statistical analysis

Data are expressed as mean±standard deviation, and statistical significance of single factor variables was assessed using one-way ANOVA, followed by Dunnett's *t*-test.  $P < 0.05$  was considered to be statistically significant, and all analyses were carried out using SAS 8 statistical software for data analysis.

### Results:

#### 1. General observations and mortality

On the day of the operation, each animal exhibited reduced feeding, drinking and activities, but their parameters improved significantly the following day. After surgery, the SAH group had slightly increased feeding, drinking, and weight, but decreased

activity, compared with the control group, but these changes were not statistically significant. Blood gas analysis revealed no significant differences in the indices; with the average values of PaCO<sub>2</sub> 4.5±0.2 kPa, and PaO<sub>2</sub> 13.7±0.5 kPa. There was also no difference in the temperatures of the mice. The mortality in each group was as follows: 0% control group (0/18), 0% in the SAH 1d group (0/18), 5.56% in the SAH 3d group (1/18), 11.11% in the SAH 5d group (2/18), 11.11% in SAH 7d group (2/18), and 11.11% in the SAH 14d group (2/18).

#### 2. Morphological detection

##### 2.1 General observations

No blood was found in the subarachnoid of the control group. However, one day after SAH, the surface of the brain exhibited subarachnoid hemorrhage. After 3 and 5 days, the surface of the brain had obvious subarachnoid hematocele, particularly after 3 days, with blood in the base of the brain, predominantly concentrated around the basilar cistern and basilar artery. After 7 and 14 days, the subarachnoid hematocele had absorbed, and was only scattered around the visible presence of the basilar cistern and basilar artery arachnoid with a yellow dye (Fig. 1).

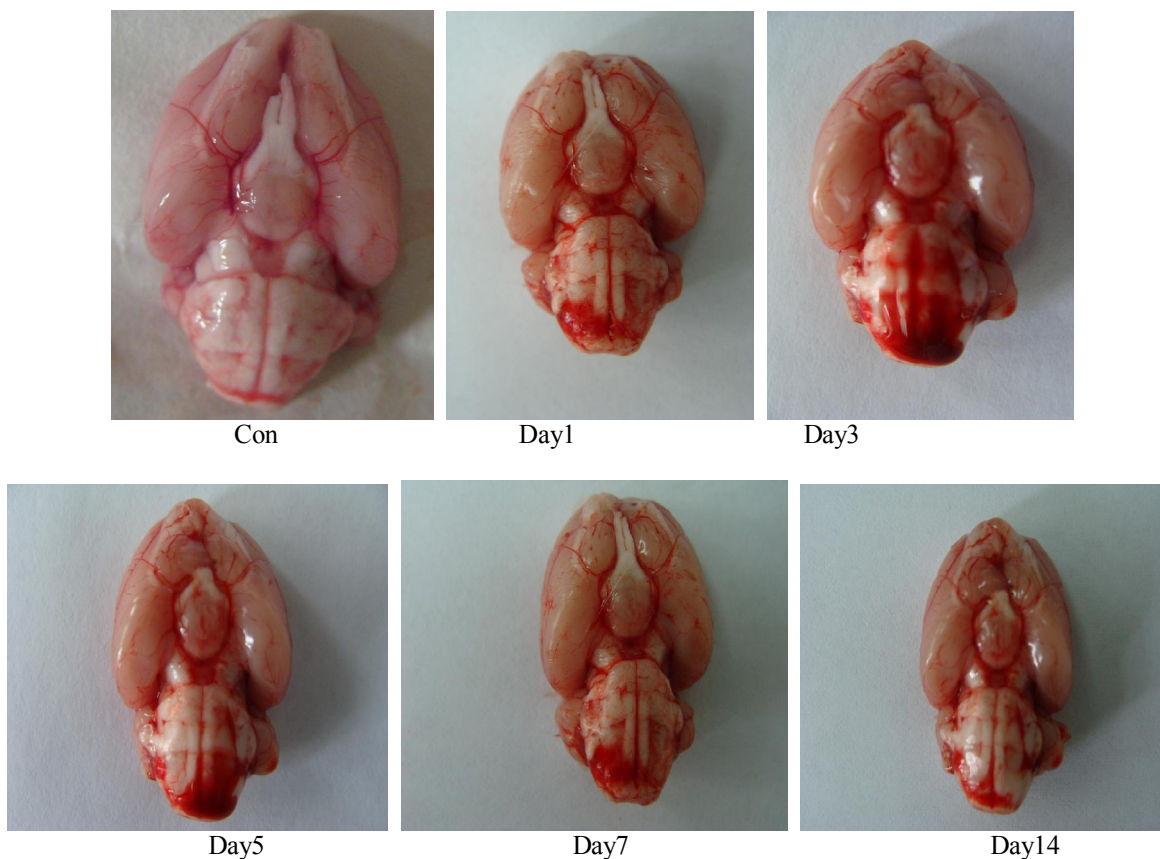


Figure1: Examples of subarachnoid hemorrhages

## 2.2 Light microscopy

The morphology of the basilar artery was next assessed by light microscopy. In the control group, the artery had a thinner vascular wall and smooth lumen, while endothelial cells exhibited no necrosis or detachment, formed a continuous single cell layer, and the nuclei had no pyknosis. The internal elastic layer also exhibited no shrinkage or rupture. The vascular smooth muscle walls were flat, with complete cell organ. However, cells from the SAH1d-7d group exhibited altered basilar artery structure, with vascular wall incassation, narrow lumens, and a disordered structure. In addition the endothelial cells were deformed and swollen, with a shrunk and tortuous internal elastic membrane of uneven thickness. Smooth muscle cells were also disordered, with increased

extracellular matrix, and inflammatory cells in the underintrima and outer membrane. In contrast, the 14d group basilar artery structure had no obvious changes. The pathological changes in the SAH-3d and 5d group were obvious, with narrow lumen and incassated lumen wall, while some endothelial necrosis disrupted the internal elastic layer, leading to the formation of cytoplasmic vacuoles, nuclear chromatoid and pycnosis, and a shrunken and ruptured internal elastic layer. In addition SMC were hypertrophied, degenerated and necrotic, with an obviously thicker membrane. In the SAH 7d and 14 day groups the narrowing of the lumen is alleviated, vascular walls were thinner, endothelial cells were deformed, desquamated, the internal elastic layers exhibited light crimples, but the hypertrophy and distortion of the SMC were alleviated (Fig. 2).

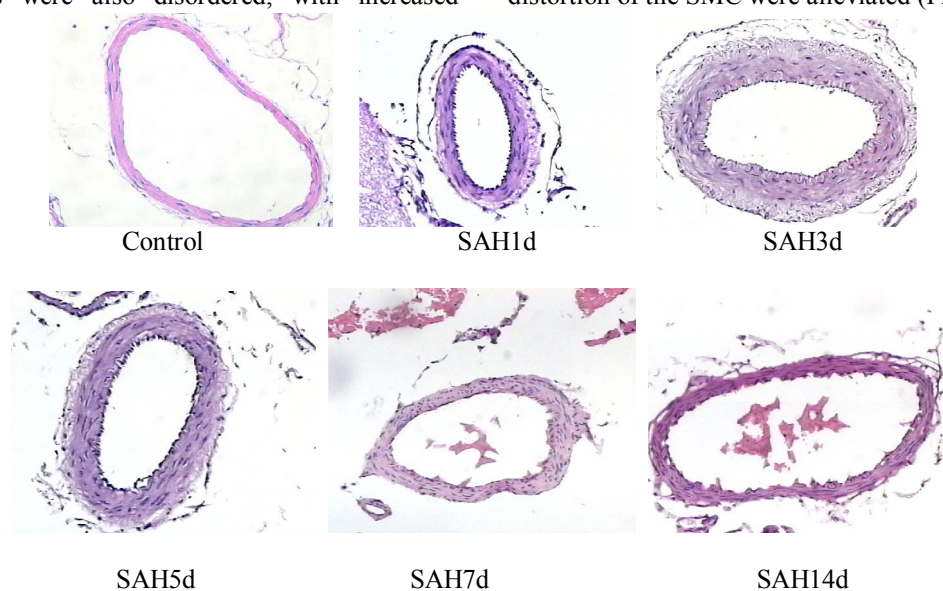


Figure 2. Haematoxylin and Eosin staining of the rat basilar artery

## 2.3 The BA cross-sectional area

The cross-sectional area of the BA in the control group was  $57,944 \pm 5,581 \mu\text{m}^2$ . The BA in the SAH1d and groups were narrowed compared with the control group, with a mean cross-sectional area of  $32,100 \pm 2,439 \mu\text{m}^2$  and  $19,723 \pm 2,412 \mu\text{m}^2$ ,

respectively. The effects were then exacerbated in the SAH5d group to  $26,100 \pm 2,639 \mu\text{m}^2$ . In the SAH7d and SAH14d groups, the stenosis was obviously alleviating, with areas of  $34,800 \pm 2,580 \mu\text{m}^2$ , and  $57,100 \pm 2,579 \mu\text{m}^2$ , respectively (Figure 3).

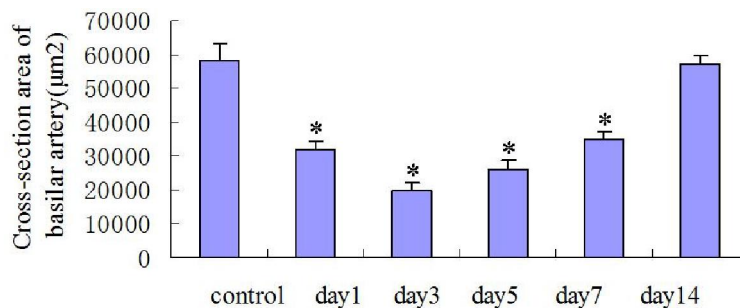


Figure 3 Comparison of the cross-sectional areas of the basilar artery (\* $P < 0.05$  vs. control)

### 3 Immunohistochemistry of TRPC1 and TRPC4 in the BA vessel wall

The BA vessel walls of the control group exhibited few or no cells that were positive for phosphorylated TRPC1 and TRPC4. In contrast, the SAH group had increased positive staining in the endomembrane and SM layer, but little expression in the outer layer. Semi-quantitative analysis of the data revealed mean staining scores as follows: TRPC1; control group (0.40), SAH1d (2.20), SAH3d (3.40), SAH5d (3.10), SAH7d (2.57), and SAH14d (0.50).

TRPC4 staining: control (0.43), SAH1d (2.21), SAH3d (3.37), SAH5d (3.21), SAH7d (2.57), and SAH14d (0.45). Compared with the control group, the expression of TRPC1 and TRPC4 was increased significantly in the BA vessel wall of each SAH group ( $P < 0.05$ ). The increase was most pronounced in the SAH3d group compared with the SAH7d group ( $P < 0.05$ ). The expression of TRPC1 and TRPC4 in the vessel walls is then decreased from day 5, recovering to baseline levels by day 14 (Figures.4, 5, 6, 7).

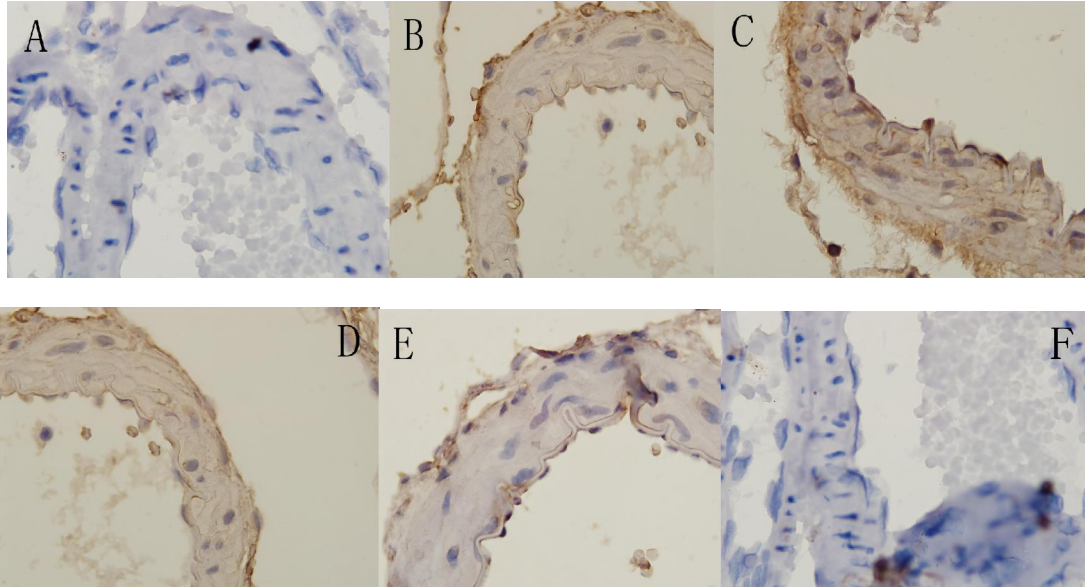


Figure 4. TRPC1 expression in the BA vessel wall, assessed by immunohistochemistry (A: control, B: SAH1d, C: SAH3d, D: SAH5d, E: SAH7d, F: 14d)

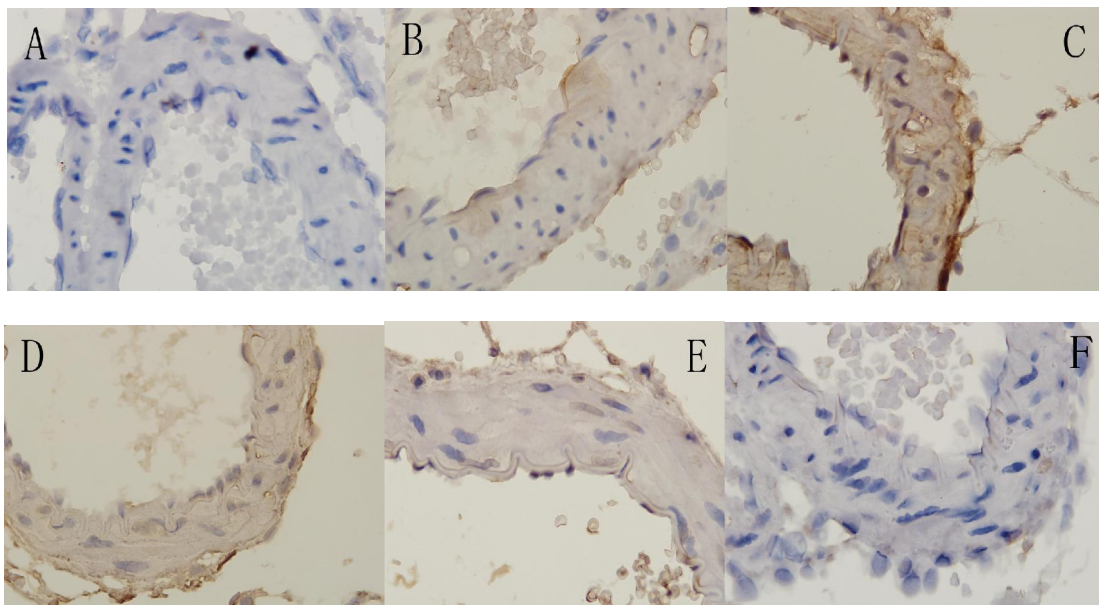


Figure 5. TRPC4 expression in the BA vessel wall, assessed by immunohistochemistry (A: control, B: SAH1d, C: SAH3d, D: SAH5d, E: SAH7d, F: 14d)

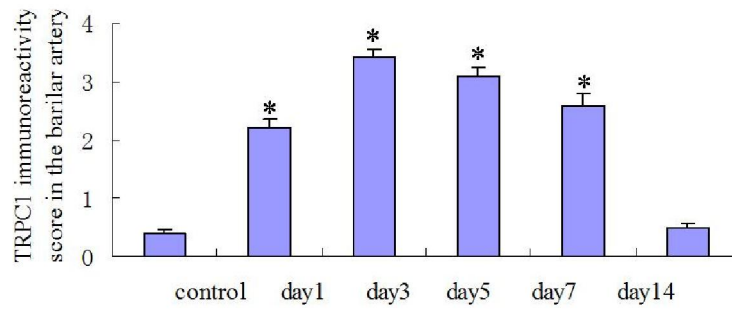


Figure 6. Quantitation of the phosphorylation of TRPC1 in the BA vessel wall (\* $P < 0.05$  vs. control)

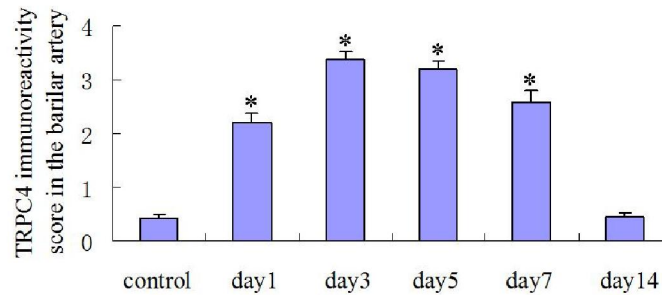


Figure 7. Quantitation of the phosphorylation of TRPC4 in the BA vessel wall (\* $P < 0.05$  vs. control)

**4 TRPC1 and TRPC4 mRNA Expression in the BA vessel wall, assessed by PCR amplification**

Very low levels of TRPC1 and TRPC4 mRNA expression were detected in the control group. In contrast, expression was increased in the SAH groups peaking at day 3, and then declining. Compared with

control, the mRNA expression of TRPC1 and TRPC4 was increased significantly in the SAH groups ( $P < 0.05$ ). In addition, the expression in the SAH3d, and 5d groups were increased significantly compared with SAH7d and SAH14d groups ( $P < 0.05$ ; Figs. 8, 9).

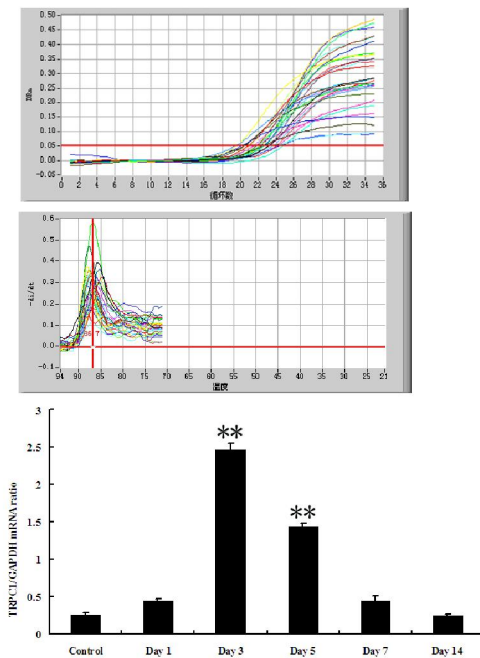


Figure 8. TRPC1 mRNA expression.

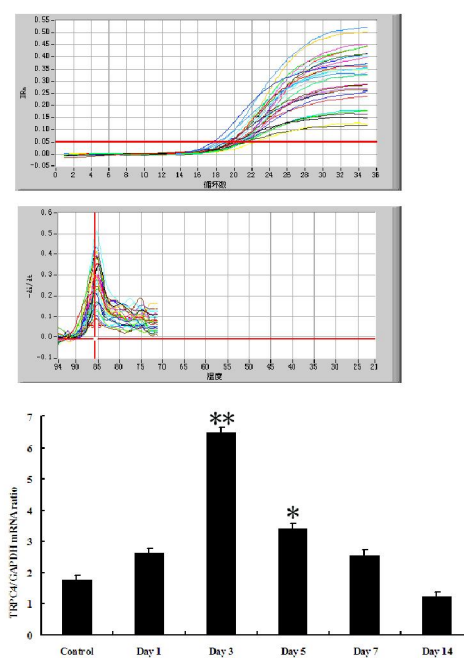


Figure 9 TRPC4 mRNA expression

### 5 The expression of TRPC1 and TRPC4 in the BA vessel wall, assessed by western blotting

Low levels of expression of TRPC1 and TRPC4 were detected in the control group. Consistent with the mRNA data, each SAH group expressed significantly higher levels, starting at day 1, peaking at day 3, and then descending, recovering to normal by day 14. Compared with control, each SAH group had significantly increased expression of TRPC1 and TRPC4 ( $P < 0.05$ ). In addition, the SAH3d and 5d groups were significantly different from the SAH7d and SAH14d groups ( $P < 0.05$ ; Figs. 10, 11, 12)

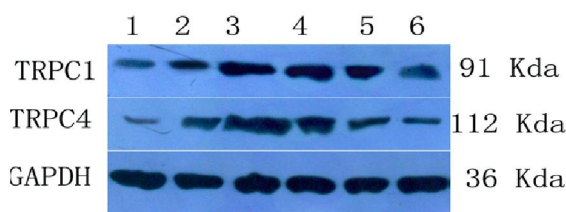


Figure 10. The expression of TRPC1 and TRPC4 in the BA vessel wall, as assessed by immunoblotting

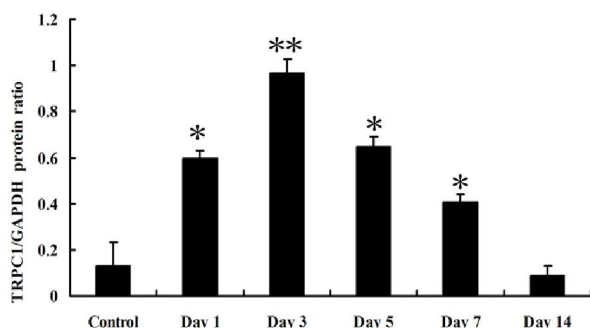


Figure 11 Quantification of TRPC1 expression in BA vessel walls (\* $P < 0.05$  vs. control)

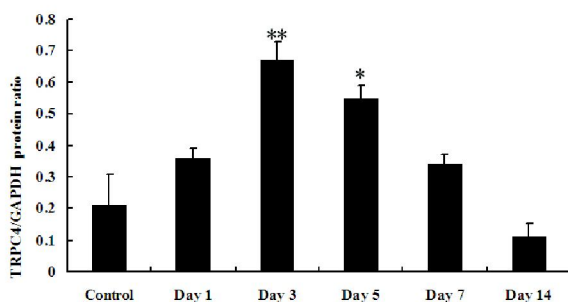


Figure 12 Quantification of TRPC4 expression in BA vessel walls (\* $P < 0.05$  vs. control)

### Discussion

Cerebral vasoplasm after aneurismal SAH is of great importance, and the subject of much research. As such, many animal models are available in which to study SAH. In 1928, Bagley *et al.* created the first SAH animal model by injecting blood into dog cisterna

magna, and many alternative models have subsequently been reported (Megyesi *et al.*, 2000; Marbacher *et al.*, 2010). Varsos *et al.* (1983) used a single injection of blood into the cisterna magna to create a dog SAH model in 1983, but no models of single injections of arterial blood into rat cisterna magna to create SAH models were reported until 1996. There are several advantages of using SD rat models using a single injection of arterial blood into the cisterna magna: 1, rats rapidly reproduce, are abundant and cheap, and feeding and maintenance after the operation is straightforward. 2, there is a high level of homogeneity between humans and rats. 3, the model accurately recreates the pathological process of biphasic vasospasm, in which the vasospasm phase is similar to clinical the human CVS process after SAH. Accidental death sometimes occurred during the experiments, predominantly due to over-anesthesia, deep punctures, or too rapid injection. Avoiding two blood injections was achieved using a tolerance control. Using this model, we observed a BA morphology that indicated obvious pathological changes after SAH, including cell degeneration, a disordered arrangement, reduced vessel lumen inner diameter, and altered vessel wall thickness. Compared with control, the SAH group exhibited a smaller inner lumen diameter, and thicker vessel wall. These changes were most prominent in the day 3 and day 5 groups, where CVS value indicated that the BA was in spasm. By day 7, the vasospasm had considerable release, comparable with previous studies (Koji and Yasuo, 2006; Takashi and Koji, 2007; Koji and Yasuo, 2010). Overall, this model is simple, gives a high success rate, and can accurately simulate the pathophysiology of CVS.

Calcium is an important intracellular second messenger, which participates in a variety of signal transduction pathways and regulates smooth muscle contractility.  $Ca^{2+}$  concentrations exist as a gradient between the extracellular matrix and cytoplasm, and intracellular calcium stores and cytoplasm. Generally, extracellular free  $Ca^{2+}$  concentrations are 100-1000  $\mu\text{mol/L}$ , which is 3-4 orders of magnitude higher than resting cytoplasmic  $Ca^{2+}$  concentrations. Upon cellular excitation, a small quantity of extracellular  $Ca^{2+}$  enters cytoplasm, significantly increasing cytoplasmic  $Ca^{2+}$  concentrations, and generating  $Ca^{2+}$  signals. During excitation, intracellular  $Ca^{2+}$  stores also release  $Ca^{2+}$  into cytoplasm, further increasing the intracellular  $Ca^{2+}$  signal. The  $Ca^{2+}$  channel is the main channel by which extracellular  $Ca^{2+}$  enters the cell, and regulates vascular smooth muscle contraction by controlling intracellular  $Ca^{2+}$  concentrations.  $Ca^{2+}$  channels can be classified based on their activation pattern, and are divided into voltage-dependent calcium channels (VDCC) and non-VDCC. Non-VDCC channels include store-operated  $Ca^{2+}$  entry channels (SOCC), receptor-

operated  $\text{Ca}^{2+}$  entry channels (ROCC), and mechanosensitive  $\text{Ca}^{2+}$  entry channels (MSCC) (William and Odile, 2000; Parekh and Putney, 2005).

Generally, intracellular  $\text{Ca}^{2+}$  concentrations are approximately 0.1  $\mu\text{mol/L}$ , but can reach higher than 1  $\mu\text{mol/L}$  after a cell has been excited. The increase in  $\text{Ca}^{2+}$  can regulate the function of various proteases and ion channels. Importantly,  $\text{Ca}^{2+}$ -ATP enzymes and  $\text{Ca}^{2+}$  pumps restore  $\text{Ca}^{2+}$  levels to normal, avoiding high  $\text{Ca}^{2+}$  levels that could cause cellular damage. Because  $\text{Ca}^{2+}$  pumps are located in the cell membrane and endoplasmic reticulum, cytoplasmic  $\text{Ca}^{2+}$  can enter the endoplasmic reticulum, or exit the cell. IP<sub>3</sub>-stimulated  $\text{Ca}^{2+}$  release therefore exhausts intracellular  $\text{Ca}^{2+}$  stores. If the IP<sub>3</sub> receptor is activated, specific SOCC or ROCC  $\text{Ca}^{2+}$  channels in the cell membrane are opened, and extracellular  $\text{Ca}^{2+}$  enters the cytoplasm to restore intracellular calcium concentrations. Putney described the concept of capacitive  $\text{Ca}^{2+}$  -entry, CEE, hypothesizing that  $\text{Ca}^{2+}$  influx resulted in exhaustion of endoplasmic reticulum  $\text{Ca}^{2+}$  supplies (Putney, 1986). Since 1989, the existence of SOCC was confirmed using electrophysiology (Venkatachalam et al., 2002; Stuart and Robert, 2009; María and Isabel, 2012). However, because no selective channel blockers were available, the progress of research into the structure and function of non-selective ion channels such as ROCC and SOCC has been slow. However, the identification of the transient receptor potential (TRP), which belong to the family of positive ion channels, allowed increased research in this area.

TRP channels represent a novel approach by which  $\text{Ca}^{2+}$  intake plays a vital role in transmitting extracellular signals. Because TRP channels have relatively low electrical conductivity, they can transmit long-term calcium signals, modulating cellular activities including smooth muscle contraction and cellular proliferation (Obukhov and Nowycky, 2002). Transient receptor potential (TRP) is a transmembrane protein that (when excited) allows positive ions, including calcium, to be transported across the membrane. The TRP channel protein was first identified in the photoreceptors of fruit flies with a TRP gene mutation. The TRP super-family can be divided into 3 sub-families with homologous genes: canonical TRP, TRPM (melastatin-related TRP)和, and TRPV (vanilloid-related TRP). TRPC channels have a 6-transmembrane hydrophobic structure, with the N- and C-terminal regions in the cytoplasm, and a non-selective positive ion channel consisting of 5 or 6 transmembrane domains. The TRPC forms a channel between segments 5 and 6. Because segment 4 lacks a common positively charged amino acid, the TRPC channel is non-voltage-gated. The first TRP channel identified was TRPC, and a total of seven TRPC sub-families have been identified, named TRPC1-7.

TRPC constitutes the major TRP family, and is widely expressed in mammals. G protein-coupled receptors or TRKs can activate the TRPC channel sub-family by regulating PLC. Activated PLC can then hydrolyze PIP<sub>2</sub> to form IP<sub>3</sub> and DAG, resulting in the release of IP<sub>3</sub>-sensitive calcium stores. This results in the activation of TRPC channels, allowing the influx of calcium into the cytoplasm to maintain calcium stores (Xi et al., 2008). The function of the TRPC sub-family was thought to be SOCC, until studies identified TRPC channels that could be directly activated by DAG, named ROCC. TRPC can therefore be activated by G protein-coupled receptors, RTK-induced PLC channels, or intracellular calcium ion concentrations (Jeremy and Wayne, 2006).

TRPC1 is widely expressed in vascular smooth muscle cells. It may play a role in SOCC, by forming pores, or directly regulating SOCC. Overexpressing TRPC1 increases calcium influx and vasoconstriction due to the exhaustion of intracellular calcium stores. In contrast, the specific antigen combines with TRPC1 channels or SOCC, inhibiting endothelin-1-induced arterial constriction (Targher and Bertolinic., 2005). TRPC1 channels are expressed on cell membranes and the endoplasmic reticulum of smooth muscle cells, and play an important role in contraction. Alfonso et al reported that TRPC1 homopolymers on the surface of the cell membrane were not functional (Alfonso et al., 2008). The subunits must combine with TRPC4 to form hetero-oligomers capable of inducing the influx of cations. However, TRPC1 homopolymers can form functional channels on the surface of the endoplasmic reticulum, and are regulated by the IP<sub>3</sub> signal transduction cascades, suggesting that TRPC1 is a multifunctional protein. TRPC1 homopolymers play a role in building ion channels that release calcium in the endoplasmic reticulum, but also form TRPC1/TRPC4 hetero-oligomers in ion channels. On the membrane of smooth muscle cells, TRPC1 may therefore have synergistic effects on the expression of TRPC4. Additional studies revealed that TRPC1 could regulate the proliferation of vascular smooth muscle cells(Kumar et al.,2006), since increased expression of TRPC1 was detected in new neointima smooth muscle cells after vascular injury. In addition treating with TRPC1 antigen inhibited the proliferation of endometrial cells after injury, whereas Lin et al reported that SOCC and ROCC were inhibited when siRNA (small interfering RNA) was used to decrease the expression of TRPC1 and TRPC2. They therefore hypothesized that TRPC1 and TRPC2 may form the molecular basis of SOCC and ROCC (Lin et al., 2004). In different cell populations in which SOCC is present, the expression of TRPC1 remains constant (J Moneer et al, 2005). TRPC1 expression is regulated by stromal interaction molecule 1 (STIM1), which is a calcium

binding protein in the endoplasmic reticulum. STIM1 combines specifically with TRPC1 and TRPC4 to form calcium receptors. The depletion of calcium pools in endoplasmic reticulum results in the accumulation and migration of STIM1 towards membrane, allowing the ERM domain (ezrin-radixin-moesin) to combine with TRPC1 at the C-terminus of STIM1 (a lysine-rich region that plays a role in the gated progress of TRPC1/SOCC), confirming that TRPC1 partially constitutes SOCC. Taken together, these data suggest that TRPC1 and TRPC4 play an important role in the regulation of vascular smooth muscle contraction.

Overall, the TRCP subfamily plays an important role in ROCC and SOCC store-operated channels, leading to contraction of cerebral vascular smooth muscle (Xi et al., 2008). Although TRCP channels are highly expressed in the central nervous system, there have been no studies of the effects of TRCP1 and TRCP4 after SAH in the CVS.

In this study, we used immunohistochemistry, PCR, and western blotting to assess the expression of TRCP1 and TRCP4 in the basilar artery in a rat experimental model of SAH. We found that the expression of TRPC1 and TRPC4 is increased in both endothelial cells and smooth muscle cells after SAH, predominantly in the cytoplasm and cell membrane. The elevated expression of both proteins was detected after SAH on day 3, peaked on day 5, but started to decline on day 7. This is consistent with the progress of arterial narrowing, the thickness of arterial wall, and the degeneration of endothelial cells and smooth muscle cells. PCR and western blotting analysis also revealed that the expression of TRPC1 and TRPC4 was maintained between days of 3-5, but then dropped and eventually normalized by day 14. The expression of TRCP1 and TRCP4 was therefore closely connected with changes in cerebral vascular pathology and cerebral vasoplasm. It is therefore possible that the activation of TRCP1 and TRCP4 is associated with the pathogenesis of CVS, and that the activation of TRCP subfamily channels triggers the transmembrane transport of calcium ions, via both ROCC and SOCC. The activation of smooth muscle contraction regulates signal transduction pathway, which leads to the contraction of cerebral vascular smooth muscle. As a result, TRPC1 and TRPC4 factors play an important role in cerebral vasospasm after SAH.

#### **In Conclusion:**

In this study, the rat "double-hemorrhage" model of vasospasm was successfully induced. The changes in the basilar artery were apparent on day 3, characterized by arterial narrowing, reduced thickness of arterial wall, and the degeneration of endothelial and smooth muscle cells, suggesting specific CVS effects after SAH. The expression of TRPC1 and TRPC4 are increased after SAH, which is correlated with the

pathogenesis of CVS. This suggests that TRPC1 and TRPC4 may regulate the development of CVS, although the mechanism for these effects remains unclear.

#### **Acknowledgements:**

This work was supported by grants from the National Natural Science Foundation of China (81371279).

#### **Corresponding Author:**

Zhong Wang,  
Department of Neurosurgery,  
The First Affiliated Hospital of Soochow University,  
Suzhou, Jiangsu Province, China  
Email:[Dr.zhongwang@gmail.com](mailto:Dr.zhongwang@gmail.com)

#### **References:**

- [1] Dumont AS, Dumont RJ, Chow MM, et al. Cerebral vasospasm after subarachnoid hemorrhage: putative role of inflammation. *Neurosurgery*, 2003; 53(1):123-33.
- [2] Ali A, Adam W, Navneet M, et al. Outcome Following Symptomatic Cerebral Vasospasm on Presentation in Aneurysmal Subarachnoid Hemorrhage: Coiling vs. Clipping. *World Neurosurgery*, 2010; 74(1):138-142.
- [3] Gregory JV, Matthew M, Kimball JD, et al. Vasospasm After Aneurysmal Subarachnoid Hemorrhage: Review of Randomized Controlled Trials and Meta-Analyses in the Literature. *World Neurosurgery*, 2011; 76(5): 446-454.
- [4] Kassell NF, Torner JC, Haley EC, et al. The International Cooperative Study on the Timing of Aneurysm Surgery. Part I: Overall management results. *J Neurosurg*, 1990; 73(1):18-36.
- [5] Yahia ZA, Nicolas MO, Audrey CQ, et al. A Review of Delayed Ischemic Neurologic Deficit Following Aneurysmal Subarachnoid Hemorrhage: Historical Overview, Current Treatment and Pathophysiology. *World Neurosurgery*, 2010; 73(6): 654-667.
- [6] Christos L, Neeraj N. Risk Factors and Medical Management of Vasospasm After Subarachnoid Hemorrhage. *Neurosurgery Clinics of North America*, 2010; 21(2):353-364.
- [7] Harders A, Kakarieka A, Braakman R. Traumatic subarachnoid hemorrhage and its treatment with nimodipine. *Journal of Neurosurgery*, 1996; 85(1):82-89.
- [8] Ville S, Petros NK, Timo K, et al. A Randomized Outcome Study of Enteral versus Intravenous Nimodipine in 171 Patients After Acute Aneurysmal Subarachnoid Hemorrhage. *World Neurosurgery*, 2012; 78(1-2):101-109.
- [9] Dorsch NW. A review of cerebral vasospasm in aneurysmal subarachnoid haemorrhage: Part II: Management. *Journal of Clinical Neuroscience*, 1994; 1(2):78-92.
- [10] Dietrich HH, Dacey RG. Molecular keys to the problems of cerebral vasospasm. *Neurosurgery*, 2000; 46(3):517-30.
- [11] Xu DZ, Yi TZ, Yi W, et al. Potential role of Ras in cerebral vasospasm after experimental subarachnoid hemorrhage in rabbits. *Journal of Clinical Neuroscience*,

- 2010;17(11):1407-1411.
- [12] Ricardo J.K, Brad EZ, Ricky V, et al. Advances in vasospasm treatment and prevention .Journal of the Neurological Sciences, 2007; 261(1-2):134-142.
- [13] Shigeru N, Ismail L. Signaling Mechanisms in Cerebral Vasospasm .Trends in Cardiovascular Medicine, 2005; 15(1): 24-34.
- [14] Yao XQ, Garland CJ. Recent developments in vascular endothelial cell transient receptor potential channels. *Cric Res*, 2005;97:853—863.
- [15] Daniela D, Baruch M. Cellular functions of Transient Receptor Potential channels .The International Journal of Biochemistry & Cell Biology,2010;42(9):1430-1445.
- [16] Yoon HC, Daejin K. Immunohistochemical study on the distribution of canonical transient receptor potential channels in rat basal ganglia.*Neuroscience Letters*, Volume 422, Issue 1, 5 July 2007, Pages 18-23.
- [17] Salgado A, Ordaz B. Regulation of the cellular localization and function of human transient receptor potential channel 1 by other members of the TRPC family .*Cell Calcium*, 2008;43(4):375-387.
- [18] Alexander D, Vladimir C. Cation channels of the transient receptor potential superfamily: Their role in physiological and pathophysiological processes of smooth muscle cells .*Pharmacology & Therapeutics*, 2006; 112(3): 744-760.
- [19] Geoffrey EW, Stewart OS. Transient Receptor Potential Channels and Intracellular Signaling .*International Review of Cytology*, 2007; 256: 35-67.
- [20] Ambudkar IS, Liu X, Paria B. Transient Receptor Potential Channels.*Encyclopedia of Biological Chemistry*, 2013; 3(1):412-417.
- [21] Park IS, Joseph RM. Subarachnoid hemorrhage model in the rat: Modification of the endovascular filament model .*Journal of Neuroscience Methods*, 2008; 172(2):195-200.
- [22] Livak KJ, Schmittgen TD. Analysis of relative gene expression data using real-time quantitative PCR and the 2(-Delta Delta C(T)) Method. *Methods* 2001; 25:402-408.
- [23] Liu WH, David A. Saint Validation of a quantitative method for real time PCR kinetics. *Biochemical and Biophysical Research Communications*, 2002; 294:347–353.
- [24] Megyesi JF, Vollrath B, Cook DA, et al. In vivo animal models of Cerebral vasospasm:a review. *Neurosurgery*, 2000; 46(2): 448-60.
- [25] Marbacher S, Fandino J, Kitchen ND. Standard intracranial in vivo animal models of delayed cerebral vasospasm. *Br J Neurosurg*, 2010; 24(4):415-34.
- [26] Varsos VG, Liszczak TM, Han DH, et al. Delayed cerebral vasospasm is not reversible by aminophylline, nifedipine, or papaverine in a "two-hemorrhage" canine model. *J Neurosurg*, 1983; 58(1):11-7.
- [27] Takashi I, Koji O. Activation of c-jun in the rat basilar artery after subarachnoid hemorrhage.*Neuroscience Letters*, 2007; 424(3): 175-178.
- [28] Koji O, Yasuo W. Activation of the JAK-STAT signaling pathway in the rat basilar artery after subarachnoid hemorrhage .*Brain Research*,2006;1072(9):1-7.
- [29] Koji O, Yasuo W. Oxidative stress activates STAT1 in basilar arteries after subarachnoid hemorrhage .*Brain Research*, 2010; 1332(21):12-19.
- [30] Parekh AB, Putney JW. Store-operated calcium channels.*Physiol Rev*, 2005; 85(2):757—810.
- [31] William CC, Odile CC. Properties, regulation, and role of potassium channels of smooth muscle .*Advances in Organ Biology*, 2000; 8: 247-317.
- [32] Putney JW Jr. A model for receptor-regulated calcium entry. *Cell Calcium*, 1986;7:1-12.
- [33] Venkatachalam K, van Rossum DB, Patterson RL, et al. The cellular and molecular basis of store-operated calcium entry. *Nat Cell Biol*, 2002;4:263-272.
- [34] Maria TA, Isabel MM. Privileged coupling between Ca<sup>2+</sup> entry through plasma membrane store-operated Ca<sup>2+</sup> channels and the endoplasmic reticulum Ca<sup>2+</sup> pump .*Molecular and Cellular Endocrinology*, 2012; 353(1-2): 37-44.
- [35] Stuart PM, Robert MD. Regulation of store-operated Ca<sup>2+</sup> entry in pulmonary artery smooth muscle cells .*Cell Calcium*, 2009;46(2):99-106.
- [36] Obukhov AG, Nowycky MC. TRPC4 can be activated by G-protein-coupled receptors and provides sufficient Ca<sup>2+</sup> to trigger exocytosis in neuroendocrine cells. *J Biol Chem*, 2002; 277:16172-16178.
- [37] Xi Q, Adebisi A, Zhao G, et al. IP3 constricts cerebral arteries via IP3 receptor mediated TRPC3 channel activation and independently of sarcoplasmic reticulum Ca<sup>2+</sup> release. *Circ Res*, 2008; 102(9):1118 - 1126.
- [38] Jeremy TS, Wayne ID. Emerging perspectives in store-operated Ca<sup>2+</sup> entry: Roles of Orai, Stim and TRP.*Biochimica et Biophysica Acta (BBA)* . *Molecular Cell Research*, 2006; 1763(11):1147-1160.
- [39] Targher G, Bertolinic. Non-alcoholic hepatic steatosis and its relation to increased plasma biomarkers of inflammation and endothelial dysfunction in non-diabetic men:role of visceral adipose tissue. *Diabet.med*, 2005; 22(10): 354-358.
- [40] Alfonso S, Benito O, Alicia S, et al . Regulation of the cellular localization and function of human transient receptor potential channel 1 by other members of the TRPC family. *Cell Calcium*, 2008; 43(4):375 - 387.
- [41] Kumar B, Dreja K, Shah SS,et al . Upregulated TRPC1 channel in vascular injury in vivo and its role in human neointimal hyperplasia. *Circ Res*, 2006; 98(4):557 - 563.
- [42] Lin MJ, Leung GP, WM, et al. Chronic hypoxia-induced upregulation of store-operated and receptor-operated Ca<sup>2+</sup> channels in pulmonary arterial Smooth muscle cells: a novel mechanism of hypoxic pulmonary hypertension. *Circ Res*, 2004; 95(5); 496-505.
- [43] J Moneer Z, Pino I, Emily JA,et al. Different phospholipase C-coupled receptors differentially regulate capacitative and non-capacitative Ca<sup>2+</sup> entry in A7r5 cell. *Biochem J*, 2005; 389(3):821 -829.

9/24/2013